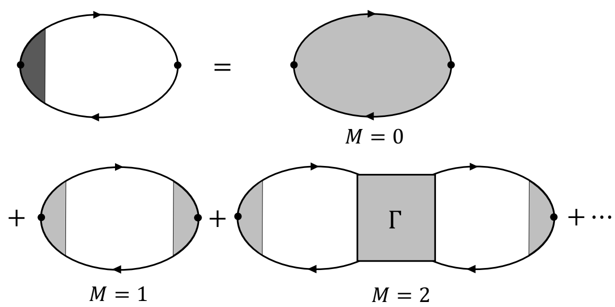

FIG. 5. The ladder series of diagrams for the static susceptibility $\chi_l^{c(s)}$. The exact χ_l is represented as a series $M = 0, 1, 2, \ldots$ of bubbles comprised of Green's functions with poles on opposite halves of the complex frequency plane, i.e. whose contributions are computed close to the FS.

pole and a branch cut. A pole can be avoided by closing the integration contour in the appropriate frequency half-plane, but the branch cut is unavoidable, and its presence renders the frequency integral finite. Since there is no splitting, relevant fermionic ω_k and $\mathbf{k}$ are not confined to the FS and are generally of order E_F (or bandwidth). Fermions at such high energies have a finite damping, i.e., are not fully coherent quasiparticles. By this reason, the $M = 0$ contribution to $\chi_l^{c(s)}$ is labeled as an incoherent one, $\chi_{l,M=0}^{c(s)} = \chi_{l,inc}^{c(s)}$ (although at small U fermions with energies of order E_F are still mostly coherent).

We next move to the $M = 1$ sector. Here we select the subset of diagrams with one cross-section, in which we pick up the contribution from $G(\mathbf{k}, \omega_k)G(\mathbf{k}+\mathbf{q}, \omega_k)$ from the range where the poles in the two Green's functions are in different half-planes of complex frequency. The sum of such diagrams can be graphically represented by the skeleton diagram in Fig. 5 labeled $M = 1$. The internal part of this diagram gives $Z^2(m^*/m)\chi_{l,0}(q)$, where $\chi_{l,0}(q)$ is given by (16). The side vertices contain $\Lambda_1^{c(s)}\lambda_l^{c(s)}(k_F)$, i.e. the product of the bare form-factor (which we already incorporated into $\chi_{l,0}(q)$), and the contributions from all other cross-sections, in which $G(\mathbf{k}, \omega_k)G(\mathbf{k} + \mathbf{q}, \omega_k)$ is approximated by $G^2(\mathbf{k}, \omega_k)$. These contributions would vanish if we used a static $U(|\mathbf{q}|)$ for the interaction, but again become non-zero once we include dynamical screening at order U^2 and higher. Similarly to the $M = 0$ sector, the difference $\Lambda_l^{c(s)} - 1$ is determined by fermions with energies of order E_F. Note, however, that in the $M = 0$ sector, all internal energies are of order E_F. In the $M = 1$ sector, internal energies for the vertices $\Lambda_l^{c(s)}$ are of order E_F, but external ω_k are infinitesimally small, and external $\mathbf{k}$ are on the FS. Overall, the contribution to the static susceptibility from the $M = 1$ sector is

$$\chi_{l,M=1}^{c(s)} = \left(Z\Lambda_l^{c(s)}\right)^2 \frac{m^*}{m}\chi_{l,0}^{c(s)} \tag{28}$$

Sectors with $M = 2$, $M = 3$ are the subsets of diagrams with $2, 3, \ldots$ cross-sections in which we split the poles of the Green's functions with equal frequencies and momenta separated by $\mathbf{q}$. In the cross-sections in between the selected ones $G(\mathbf{k}, \omega_k)G(\mathbf{k} + \mathbf{q}, \omega_k)$ is again approximated by $G^2(\mathbf{k}, \omega_k)$. The contribution from the $M = 2$ sector is represented by the skeleton diagram in Fig. 5 labeled $M = 2$. It contains fully dressed side vertices $\Lambda_l^{c(s)}$ and a fully dressed anti-symmetrized static interaction between fermions on the FS. One can easily verify that this interaction appears with the prefactor $Z^2(m^*/m)$, i.e., the extra factor in the $M = 2$ sector compared to $M = 1$ is the product of $\chi_{l,0}$ and the corresponding component of the Landau function. Using (25) we then obtain

$$\chi_{l,M=1}^{c(s)} + \chi_{l,M=2}^{c(s)} = \left(Z\Lambda_l^{c(s)}\right)^2 \frac{m^*}{m}\chi_{l,0}^{c(s)}\left(1 - F_l^{c(s)}\right) \tag{29}$$

(the minus sign comes from the number of fermion bubbles.) A simple bookkeeping analysis shows that contributions from sectors with larger M form a geometric series, which transform $1 - F_l^{c(s)}$ into $1/(1 + F_l^{c(s)})$. Collecting all contributions, we reproduce Eq. (4).

3. *The susceptibility $\chi_l^{c(s)}(\mathbf{q}, \Omega)$ at finite $\Omega/v_F^*|\mathbf{q}|$.*

We now extend the analysis to the case when both transferred momentum $\mathbf{q}$ and transferred frequency Ω are vanishingly small, but the ratio $\Omega/v_F^*|\mathbf{q}|$ is finite. The computational steps are the same as for static susceptibility. The contribution to $\chi_l^{c(s)}(q)$ from the $M = 0$ sector and the vertex function $\Lambda_l^{c(s)}$ do not depend on the ratio of $\Omega/(v_F^*|\mathbf{q}|)$ and remain the same as in the static case. However, the integrand in the expression for $\chi_{l,0}(q)$, Eq. (16), now contains a non-trivial angular dependence via $v_F|\mathbf{q}|\cos\phi_k/(\Omega - v_F|\mathbf{q}|\cos\phi_k + i\delta_\Omega)$. This makes the computation of series with $M = 1, 2, \ldots$ more involved.

Consider first the limit $\Omega \ll v_F|\mathbf{q}|$. For even l, the free-fermion susceptibility is

$$\begin{aligned}\chi_{l,0}^{c(s)}(q) &= \frac{m}{\alpha_l\pi}\left(k_F^l f_l^{c(s)}(k_F)\right)^2\left(1 + \alpha_l\frac{i\Omega}{v_F|\mathbf{q}|}\right)\\ &= \chi_{l,0}^{c(s)}\left(1 + \alpha_l\frac{i\Omega}{v_F|\mathbf{q}|}\right)\end{aligned} \tag{30}$$

where $\alpha_l = 1$ if $l = 0$ and $\alpha_l = 2$ if $l = 2m$, $m > 0$. For odd l, the expansion in Ω starts with Ω^2. The total contribution from the $M = 1$ sector still is proportional to $\chi_{l,0}$: